



This is a repository copy of *Experimental and analytical study of gear micropitting initiation and propagation under varying loading conditions*.

White Rose Research Online URL for this paper:
<http://eprints.whiterose.ac.uk/85761/>

Version: Accepted Version

Article:

Al-Tubi, I.S., Long, H., Zhang, J. et al. (1 more author) (2015) Experimental and analytical study of gear micropitting initiation and propagation under varying loading conditions. *Wear*, 328-32. 8 - 16. ISSN 0043-1648

<https://doi.org/10.1016/j.wear.2014.12.050>

Reuse

Unless indicated otherwise, fulltext items are protected by copyright with all rights reserved. The copyright exception in section 29 of the Copyright, Designs and Patents Act 1988 allows the making of a single copy solely for the purpose of non-commercial research or private study within the limits of fair dealing. The publisher or other rights-holder may allow further reproduction and re-use of this version - refer to the White Rose Research Online record for this item. Where records identify the publisher as the copyright holder, users can verify any specific terms of use on the publisher's website.

Takedown

If you consider content in White Rose Research Online to be in breach of UK law, please notify us by emailing eprints@whiterose.ac.uk including the URL of the record and the reason for the withdrawal request.



eprints@whiterose.ac.uk
<https://eprints.whiterose.ac.uk/>

Experimental and analytical study of gear micropitting initiation and propagation under varying loading conditions

I. S. Al-Tubi¹, H. Long^{1*}, J. Zhang² and B. Shaw²

¹Department of Mechanical Engineering, The University of Sheffield, United Kingdom

²Design Unit, Gear Technology Centre, The University of Newcastle, United Kingdom

*Corresponding author: Dr H. Long, email: h.long@sheffield.ac.uk

Keywords: Gears, micropitting, torque variation, surface roughness

Abstract

Micropitting damage is one of the failure modes commonly observed in gears leading to destructive failures, which in turn results in unplanned shutdown and expensive replacement, such as those observed in wind turbine gearboxes. This study investigates gear micropitting initiation and propagation when subjected to varying torque loads under a constant rotational speed. The study employs both experimental gear testing and analytical evaluation based on the ISO Technical Report of Gear Micropitting, ISO/TR 15144-1:2010 and the recently revised ISO/TR 15144-1:2014. Initiation and propagation of micropitting are assessed in testing by quantifying the development of micropits and their progressive rate after specific numbers of running cycles at step-up torque levels. The analytical study is conducted to validate the prediction of micropitting using the ISO/TR recommended procedures by comparing the results with the occurrence of micropits in the tested gears.

The gear test results show that micropitting initiates at the pinion dedendum but escalates at the addendum, because of the greater severity of progressive micropitting at the dedendum of the mating wheel where the tip relief area first comes into mesh. The analytical results, based on varying surface roughness measurements obtained from the tested gears, confirm that the maximum contact stresses and minimum specific lubricant film thicknesses occur in these regions. The specific lubricant film thickness varies considerably because of changes of surface roughness after gears are subjected to various running cycles under varying torque levels. It has found that the excessive loading, gear tooth micro-geometry, surface roughness and lubricant film thickness are the main factors affecting micropitting.

1. Introduction

Gear design and analysis methods are standardised by many international committees and manufacturing organisations, such as AGMA 2001-D04, ISO/6336 and DIN 3990, to guide the various aspects of gear design and industrial applications. The methods have been developed to investigate and eliminate gear tooth failures such as tooth breakage, surface micropitting, scuffing, sliding wear and

spalling (ISO 10825, 1995 and BS 7848, 1996). Gear tooth flanks are subjected to varying loading and relative sliding conditions when the tooth pair engages along the line of action because of changes of the radii of tooth profile curvature at different contact points and varying load sharing factors at the single/double tooth contact regions. These cause variations of some key parameters such as gear tooth contact stresses and sliding velocities between two mating teeth during each engagement cycle, especially when subjected to variable loading and variable rotational speed conditions in operation. Although gear design and failures are well studied, however, prediction of initiation and propagation of gear tooth micropitting to accurately estimate gear service life under complex operational condition is still a challenging problem. It contributes to considerable costs due to early replacement of gears, unplanned shutdowns for carrying out maintenance procedures, such as for wind turbine gearboxes.

During gear engagement, gear teeth experience a complex combination of surface rolling and sliding contact which varies along the tooth flank [1-2], as shown in Figure 1. When used as a driving gear, the pinion sliding direction is away from the pitch line, whereas the driven wheel gear slides towards the pitch line [3]. For the pinion gear, this makes the sliding motion apt to pull the material away from the pitch line. At the pitch line of the wheel gear, however, the material is compressed by the sliding motion. The dedendum of both gears has a relatively short contact length and negative sliding as the direction of the sliding velocity is in the opposite direction of the rolling velocity. Furthermore, the contact stress changes continuously throughout the meshing process and high contact stresses can occur at the single tooth contact region where the load is supported by single pair of gear teeth. The variation of contact stresses and sliding directions can cause high temperatures and mixed lubrication conditions at contact surfaces, or even break down the lubrication film along the tooth flank. In addition, the surface roughness of meshing gear teeth will change after certain running cycles under loading. This leads to variations of lubrication condition between asperities of gear contact surfaces contributing to the initiation of micropitting. Gear tooth flank micropitting is characterised by a continuous surface deterioration, owing to various operational and loading conditions. Compared to the size of the contact zone, the micropits are small and shallow, with a size of about 5–10 μm long and 5–20 μm deep [4].

Gear surface failure of micropitting is affected by many factors including gear design, material, surface treatment and finishing, lubricant, and operational conditions such as loading and velocity, and lubrication condition. The following section will briefly review the published research in micropitting and effects of these key factors.

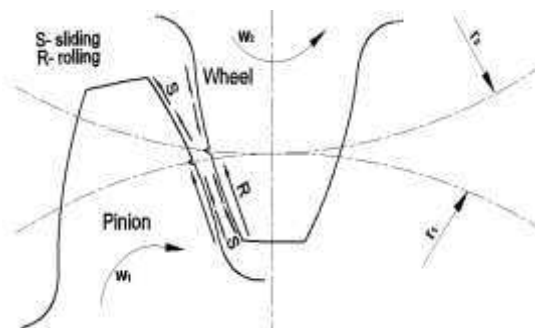


Figure 1 Gear tooth surface rolling and sliding

2. Review of recent micropitting research

Using a back-to-back gear test rig, surface durability of treated and untreated gear surfaces loaded under different torque levels was tested by Krishnamurthy and Rao [5]. The treated gears endured higher contact stresses and had a longer service life than that of untreated gears. Brechot et al [6] tested many types of gears under different load levels. The main goal of these tests was to detect the occurrence of micropitting when using different industrial lubricant oil samples. Zhang and Shaw [7] used a back-to-back gear test rig to investigate two pairs of spur gears made from the same material, but with a different surface finishing. It concluded that the superfinished gears performed better against micropitting with smaller tooth profile deviation than the ground gears. Predki et al [8] investigated micropitting of big spur gears with profile modification. Some of their key findings were that the higher surface roughness was related to wider micropitting zone, and the micropitting was influenced greatly by the amount of tip relief. Muraro et al [9] experimented with spur gears of two different surface finishes, shaving and milling, to observe the wear mechanism. Two torque levels were implemented in their tests and it was observed that the wear was lower for the shaved gears due to the effect of the lubricant film thickness. Moorthy and Shaw [10] experimentally tested helical gears with different coating compared with as-ground (uncoated) gears, using a back-to-back test rig. The authors studied the micropitting propagation and profile deviation at different torque levels and cycle numbers. Evans et al [11] analysed micro-elastohydrodynamic lubrication of two helical gears to investigate gear micropitting, using a gear test rig and predicted subsurface damage by accumulation analysis.

Hohn and Michaelis [12] tested different lubricants under different oil temperatures, and found that higher levels of micropitting were related to high contact stress and oil temperature as thin lubricant film thickness and low viscosity took place at high oil temperature. Oila and Bull [13] investigated micropitting using a two-disc machine and two different lubricant oils. One of their important conclusions was that the plastic deformation boundaries were preferred regions for micropitting initiation. Lainé et al [14] experimentally tested carburised steel rollers; one of their main findings was that the micropitting was influenced by the surface roughness and lubricant film thickness. The micropitting may be exacerbated by the use of different types of anti-wear additives. Kleemola and Lehtovaara [15] developed a twin-disc test device to investigate the effects of three parameters, friction coefficient, temperature and lubrication conditions, on micropitting. Their results showed that higher sliding led to a higher temperature increase and lower film thickness.

Holmes et al [16] used a transient analysis method to analyse lubricant film thickness in elliptical point contact, in the transverse direction. One of their key results was that the lowest film thickness occurred because of surface valleys, which helped the lubricant oil to escape between the contact surfaces in the transverse direction. Brandão et al [17] presented a numerical model and compared with a FZG testing of gear surface-initiated damages, to predict the micropitting and gear tooth wear loss. The predictions and measurement of wear losses were correlated, but the surface roughness results did not match well. Zhu and Wang [18] used different types of contact geometry and three types of contact surfaces which

were transverse, longitudinal and isotropic, to study the effect of surface roughness orientation on the EHL (elastohydrodynamic lubrication) film thickness.

Through the continuous research, the understanding of the mechanism of micropitting has been improved. However, the prediction of initiation and propagation of gear tooth micropitting to accurately estimate gear service life is still a challenging problem. This study combines the experimental and analytical studies to predict the risk of gear micropitting. In this paper, experimental and analytical methods are developed to investigate and predict the initiation and propagation of micropitting damage under varying torque levels. Surface inspection procedures, such as surface roughness measurement, replica sample and digital image analysis, and profile scanning are used on the tested pinion gear to observe the micropitting development after each cycle run at certain torque level. In addition, the ISO Technical Report of Gear Micropitting, ISO/TR 15144-1:2010 [19] and the recently revised ISO/TR 15144-1:2014 [20], are used to analyse the gear tooth contact stresses and lubricant film thicknesses at different contact points along the tooth flank of the tested gear.

3. Experimental investigation

3.1 Gear test rig

The micropitting experiment is carried out using a back-to-back gear test rig in the Design Unit of the University of Newcastle [11, 21]. The back-to-back gear test rig is designed based on a recirculating power loop principle, which provides a desired amount of fixed torque level through the tested gears, only consuming a small amount of power to drive them. The test rig is capable of testing two sets of identical gear sets with equal gear ratios. The schematic layout of the gear test rig is shown in Figure 2. Two gearboxes (A and B sets) are connected back-to-back by a flexible elastic shaft to isolate gears from any vibration and prevent them from affecting each other. Torque is applied through a van-type hydraulic torque actuator and transmitted through the shafts to the meshing gear sets A and B. The torque actuator is used in the test rig to enable the torque to be applied gradually while the rig is running and to be maintained using a close electric/hydraulic loop control mechanism. Motors are used to recycle and maintain the lubricant temperature, to provide lubrication directed at the mesh location of gear teeth. In this study, the lubricant inlet temperature is 90°C, and a computer control system is used to control the inlet temperature, torque and rotational speed.

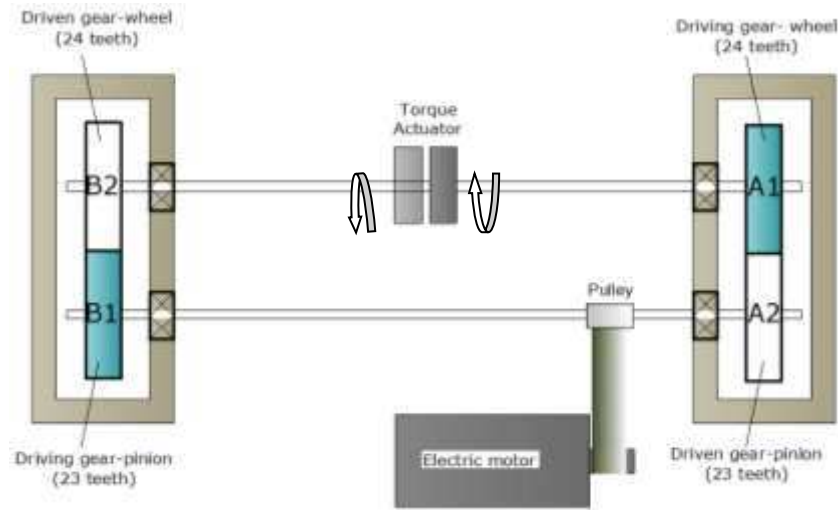


Figure 2 Schematic of the back-to-back gear test rig

3.2 Testing gears and experiment

Two pairs of helical gears are manufactured in the Design Unit of Newcastle University to perform the experiment at different levels of loading to observe micropitting initiation and progression in gear teeth. The helical gears are manufactured using the hobbing process followed by heat treatment process involving case carburising, hardening and tempering. The grinding machining process is used to finish the gear tooth flanks, with a specific geometry profile of linear tip relief and symmetrical lead crowning. Using metrology measurement to ensure high accuracy in the final grinding finishing, a very low difference between gear surfaces in surface roughness of $\pm 0.05 \mu\text{m}$ is achieved. The properties of gear material, lubricant and other parameters of the test gears are given in Table 1.

Table 1 Pinion and wheel gear parameters

Parameters	Pinion/Driver	Wheel/Driven
Number of gear teeth	23	24
Face width	44 mm	
Pressure angle	20 degree	
Helix angle	28.1 degree	
Module	6 mm	
Centre distance	160 mm	
Pitch diameter	156.44 mm	163.24 mm
Tip diameter	168.76 mm	175.24 mm
Nominal pitch line velocity	24.6 m/s	
Nominal rotational speed	3000 rpm	2875 rpm
Accuracy grade	5 (ISO 1328-1/95)	
Profile modification	Linear tip relief (0.050 mm)	

Profile shift coefficient	0.0266	0.0
Lead crowning modification	Symmetric (0.015 mm)	
Material	18CrNiMo7	
Modulus of elasticity	$207 \times 10^9 \text{ N/m}^2$	
Hardness	746 HV	
Surface hardness	Ground	
Surface roughness	$0.45 \mu\text{m} \pm 0.05 \mu\text{m}$	
Lubricant	Mineral oil with additives	
Lubricant viscosity	$320 \text{ mm}^2/\text{s}$ at $40 \text{ }^\circ\text{C}$	
	$26 \text{ mm}^2/\text{s}$ at $100 \text{ }^\circ\text{C}$	
Inlet temperature (spray lubrication)	$90 \text{ }^\circ\text{C}$	

3.3 Experimental procedure

The experiment is conducted under varying torque condition, from low to high levels, to determine at which torque level and loading cycles the micropitting occurs and propagates. For confidentiality considerations of the test programme, the varying torque values are normalised as torque ratios. To provide sufficient details of loading levels, the torque ratios and corresponding contact stress levels at gear tooth pitch point are also listed as shown in Table 2. The gears are tested under a constant rotational speed. At each torque level, a test run of 8 million cycles is performed.

The measurements of two parameters, the average surface roughness, Ra (ISO), and the mean of five heights of peak to valley, Rz (DIN), are used to observe changes of the tooth surface roughness after subjected to each load level. The surface roughness values of a single tooth of the pinion gear are measured before and after each test run of the torque levels, each of which consists of 8 million cycles. This procedure is to quantify and analyse how the gear surface roughness affects micropitting. The measured values of the tooth surface roughness are also used in the calculation of the specific lubricant film thickness in the analytical study.

In addition to the surface roughness measurements, the replicas of a tooth surface of the pinion gear are acquired after each test run of 8 million cycles, to observe the initiation and propagation of micropitting of the gear tooth flank after each loading stage. The replica samples for the tooth surface of the tested pinion are produced by injecting a replication medium onto the tooth flank after each loading level. In order to produce a good quality replica, the tooth flank is cleaned before injecting the replica medium, to remove the remaining oil and contaminants on the tooth flank. After the replica is extracted, a microscope (Nikon SMZ1500) is used to inspect the initiation and progression of the micropitting of tooth flank after each loading stage and required cycle run.

Table 2 Torque ratios and contact stress levels of the test programme

Test sequence	Cycles Number (millions)	Torque ratio	Contact stress level at pitch point
1	8	0.3	1076 MPa
2	8	0.5	1332 MPa
3	8	0.6	1452 MPa
4	8	0.7	1563 MPa
5	8	0.8	1666 MPa
6	8	0.9	1763 MPa
7	8	1	1855 MPa

At the end of the test, the gear profile deviation is measured using Hofler EMZ632 CNC gear measuring instrument to observe the maximum profile deviation and effect of micropitting. Figure 3 shows the defined points of the tip relief and the measurement of profile deviation taken in the middle of the face width on the tooth flank. Profile deviations of four teeth (number 1, 7, 13 and 19) of tested gears are measured, and the location of deviation and the extent of difference are obtained with regard to the gear geometry reference of a straight line.

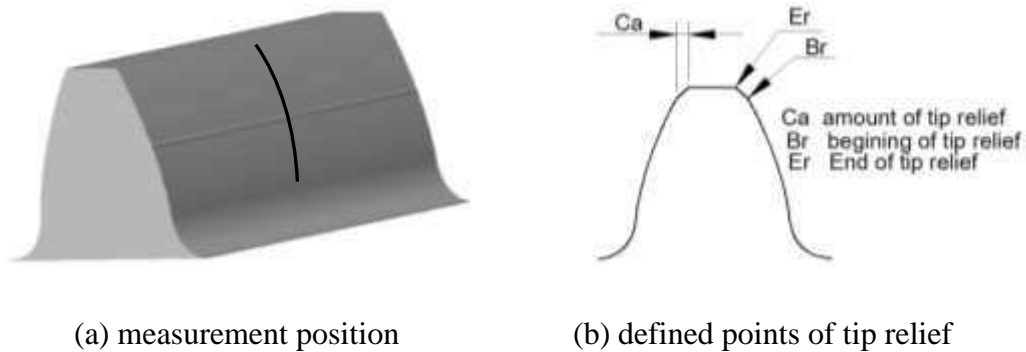


Figure 3 Gear tooth profile tip relief and deviation measurement

4. Analytical Investigation

In this study, the calculation of the tooth contact stresses and specific lubricant film thicknesses is in accordance with ISO/TR 15144-1:2010 [19] and the recently published ISO/TR 15144-1:2014 [20] and ISO 6336-1:2006 [20], by developing a toolkit calculation sheet using MS/EXCEL. The effect of symmetrical lead crowning is ignored in the analysis because the calculation is considered only at the middle of the face width where the crowning has no effect.

By applying the variable torque levels and constant rotational speed as used in the experiment and gear parameters as given in Tables 1 and 2, the contact stresses and lubricant film thicknesses can be determined. These parameters are used to assess the risk of micropitting of the tested pinion gear

(driver). Based on the ISO/TR recommended procedures [19, 20], the local Hertzian contact stress ($P_{dyn,Y}$) may be determined by Equation (1) [22]. The local lubricant film thickness (h_Y) may be estimated by Equation (2) [19, 20]. The prefix Y refers to specific points (A, AB, B, C, D, DE and E) on the tooth flank, as shown in the load sharing diagram in Figure 4. Other parameters used in the equations are explained in Nomenclature [19, 20, 22]. The meshing starts when point A (the approach point) at the root of the driving gear engages with the tip of the driven gear. The tooth tip relief is used to reduce the impact of gear teeth at meshing in/out and to enable gears operate smoothly with less vibration. Owing to the elastic deformation of loaded teeth and high sliding at tooth tips, the tip relief extensions are equal for both gears. As shown in Figure 4, the tip relief reduces the load-sharing factor in the ranges A–AB and DE–E, however increases the load-sharing factor in the range of AB–DE.

$$P_{dyn,Y} = Z_E \sqrt{\frac{F_t X_Y}{b \rho_{n,Y} \cos \alpha_t \cos \beta_b}} K_A K_V K_{H\alpha} K_{H\beta} \quad (1)$$

$$h_Y = 1600 \rho_{n,Y} G_M^{0.6} U_Y^{0.7} W_Y^{-0.13} S_{GF,Y}^{0.22} \quad (2)$$

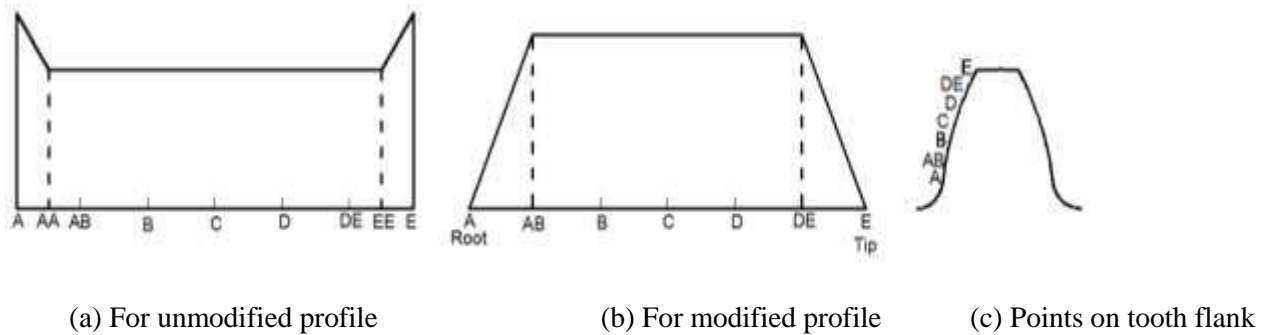


Figure 4 Load sharing of the driver gear within a meshing cycle

In the ISO/TR recommended procedures [19, 20], the specific lubricant film thickness ($\lambda_{GF,Y}$) is a dimensionless parameter, as shown in Equation (3), defined as the ratio between the lubricant film thickness (h_Y) and the mean surface roughness of meshing gears (R_a). The measurements of surface roughness are obtained from the average surface roughness (R_a) of the tested pinion gear.

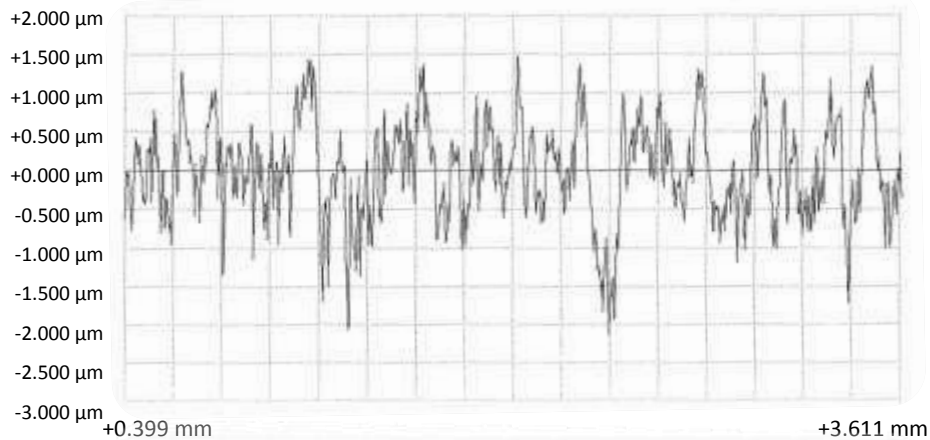
$$\lambda_{GF,Y} = \frac{h_Y}{R_a} \quad (3)$$

To validate the analytical evaluation using the ISO/TR recommended procedures [19, 20], the occurrence of micropitting in the experiment is used to assess the prediction of micropitting using the analytical method.

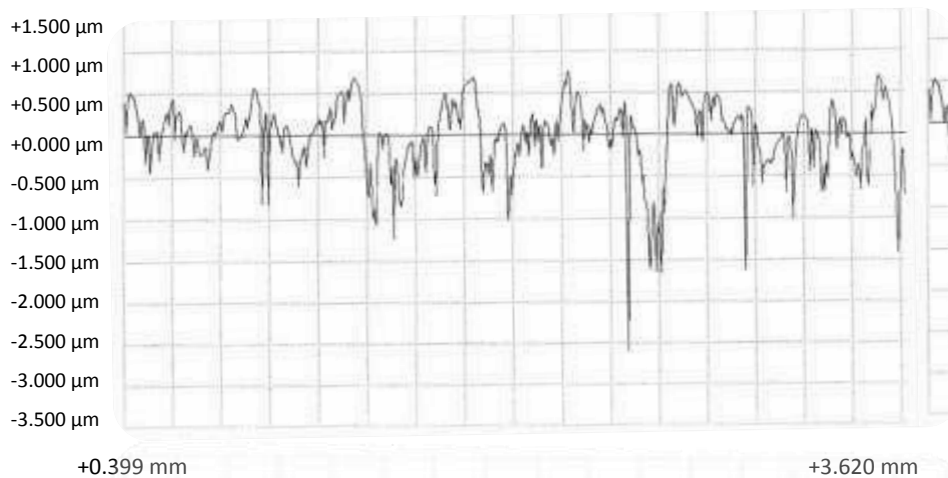
5. Experimental and analytical results

5.1 Surface roughness analysis

The comparison between the values of surface roughness measured after each test cycle run under different torque levels show that the peak values of surface asperities deteriorate, as shown in Figures 5(a) and (b). The surface roughness of pinion gear (R_a) has a steady trend of decrease with the increase of torque ratio, as shown in Figure 6 (a). However it increases slightly by about $0.01 \mu\text{m}$ at torque ratio of 0.7. This may be because of sliding motion opts to pull the material away from the pitch line as the micropitting starts to spread out. The deeper valleys of the tooth surface indicate that some material is removed from the original tooth flank due to the occurrence of micropitting. The R_z value in Figure 6 (b) shows that the peak to valley height decreases after each test cycle run. The slight increase in R_z at torque ratio 1.0 may indicate that the deep valleys are present on the tooth flank, and the difference between the peaks and valleys is increased owing to micropitting spreading on the tooth flank.

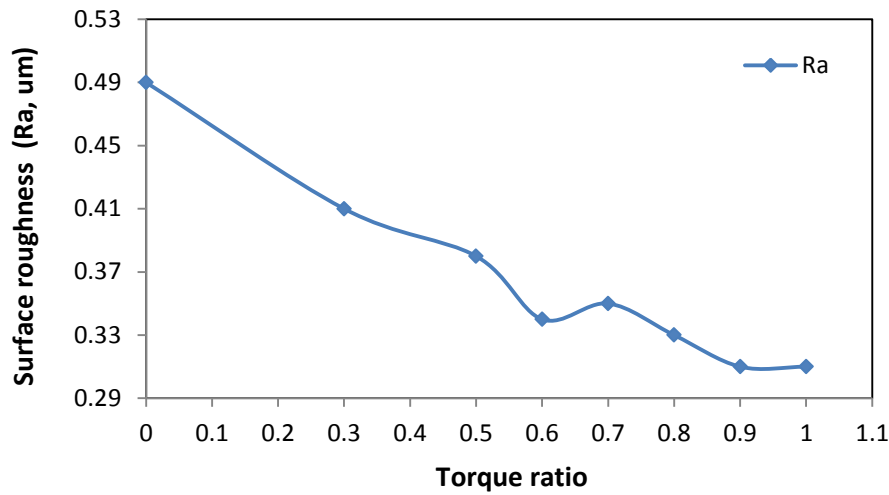


(a) Before testing (0 cycle)

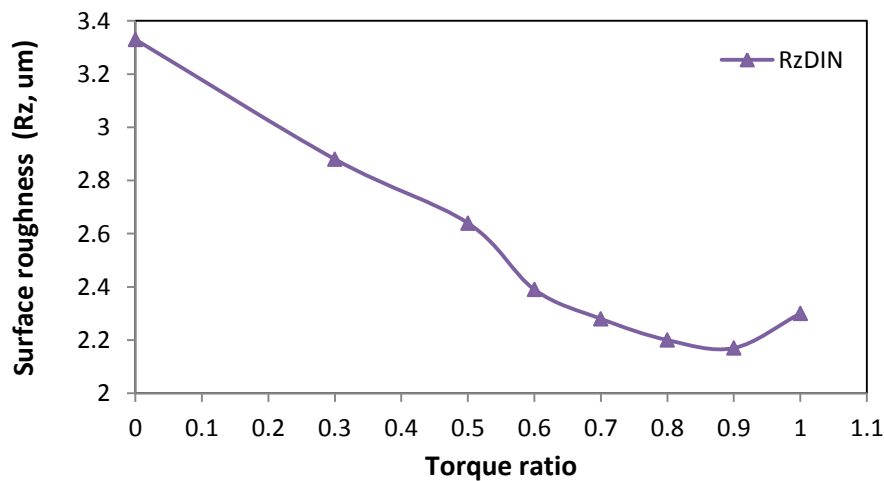


(b) After testing at torque ratio of 1.0 (56 million cycles)

Figure 5 Surface roughness measurement of pinion gear



(a) Ra values at different torque ratios



(b) Rz values at different torque ratios

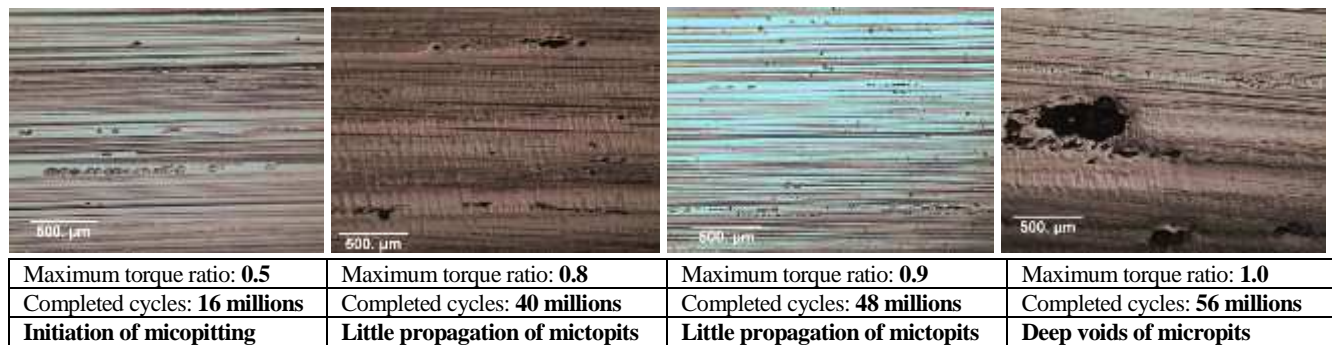
Figure 6 Surface roughness measurement results

5.2 Micropitting initiation and propagation

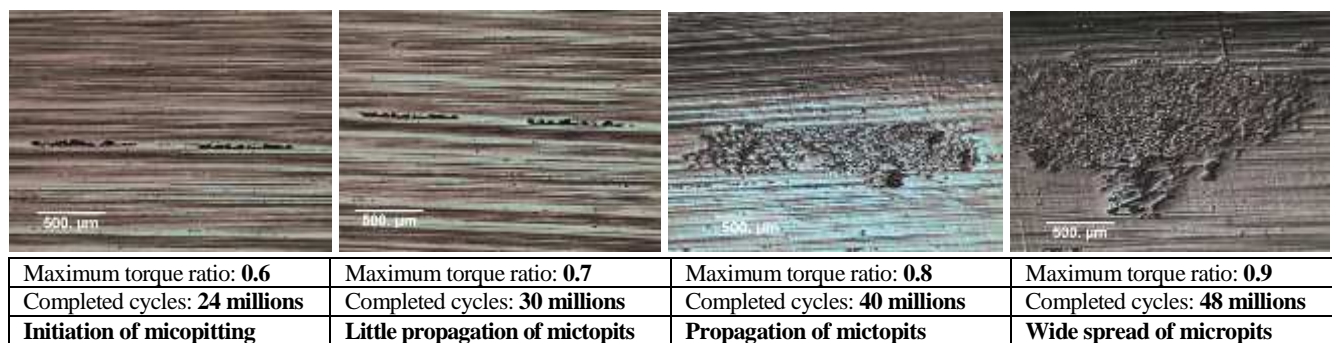
All teeth, for both pinion and wheel gears, are given engraved numbers for clear identification of locations of micropitting. The gear surface replicas of pinion tooth 1 are produced and microscopic inspection is performed at all test stages to study the micropitting occurrence and development at different torque levels, as shown in Figure 7. At the torque ratio of 0.3, no micropitting is observed. At the torque ratio of 0.4 a micropit occurred at the dedendum of pinion, however, this micropit is non-progressive and occurs infrequently along the dedendum area until the end of the test, as shown in Figure 7 (a). The micropitting initiates at the addendum at a higher torque ratio of 0.6, however, it propagates densely and progressively when the high torque ratios are applied, as shown in Figure 7 (b). The cause of this is that the micropitting is initiated at the dedendum of wheel where the grinding cutting edges exist due to the tooth profile tip relief, which meshes with the addendum of pinion thus causing the progressive micropitting in the addendum area of pinion. At the end of the test, the

micropitting spreads out on most of the tooth surface at various locations, in both addendum and dedendum of the wheel. The micropitting spreads out at both addendum and dedendum of the pinion tooth flank towards the end of test at torque ratios of 0.9 and 1.0, also observed by Brechot et al [6] and Snidle et al [23]. However, though the micropitting area at the pinion dedendum is smaller than that at the addendum area, pits occurred are deeper at the dedendum area, which will be explained in the profile deviation results.

Figure 8 shows how the micropitting spreads out on the tooth flank of the pinion and wheel at the end of the test after being subjected to different levels of loading. Dudley (1) suggested that the pitting can occur at the addendum area of a driven wheel due to the severe load. As shown in Figure 8, the wheel has more progressive micropitting at the dedendum area, and it almost covers about 60–70 % of the wheel dedendum along the face width, thus the addendum of pinion gear is prone to more progressive micropitting. The observation reveals that the micropitting can initiate at the dedendum and/or at the addendum, but the area of fast propagation can trigger the initiation of micropitting of the mating tooth surface. Table 3 summarises the initiation and propagation of micropitting under different torque ratios.



(a) Pinion gear tooth dedendum



(b) Pinion gear tooth addendum

Figure 7 Micropitting initiation and propagation under different torque ratios and load cycles

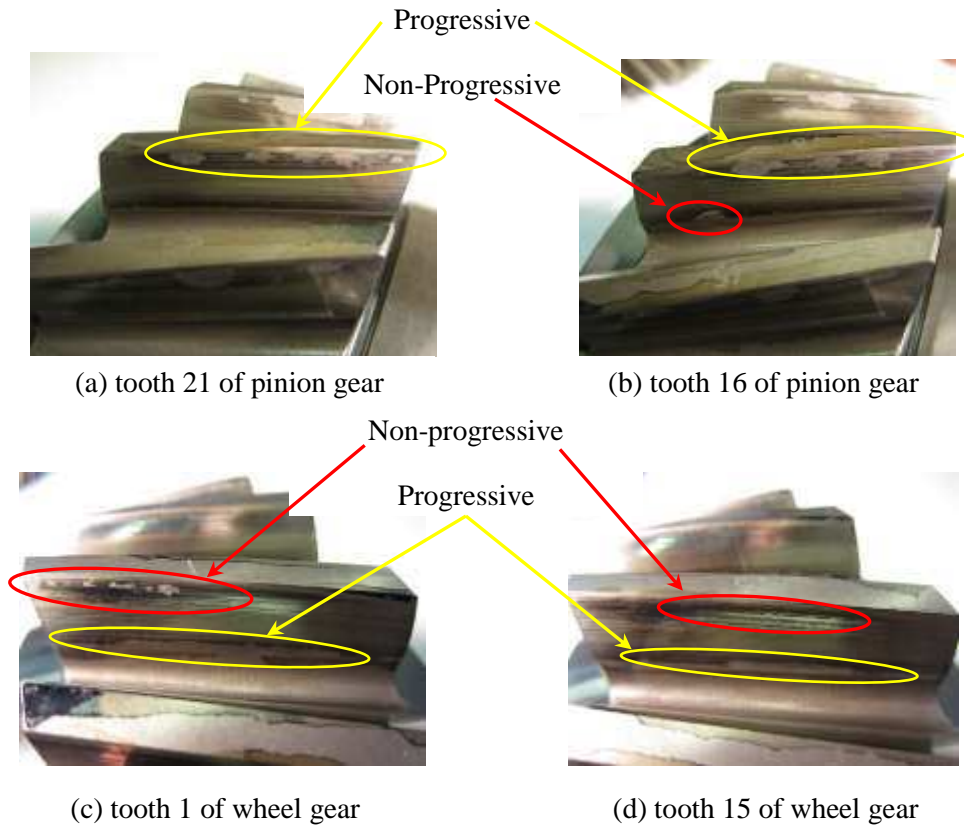


Figure 8 Propagation of gear tooth micropitting

Table 3 Summary of the micropitting propagation under different torque ratios

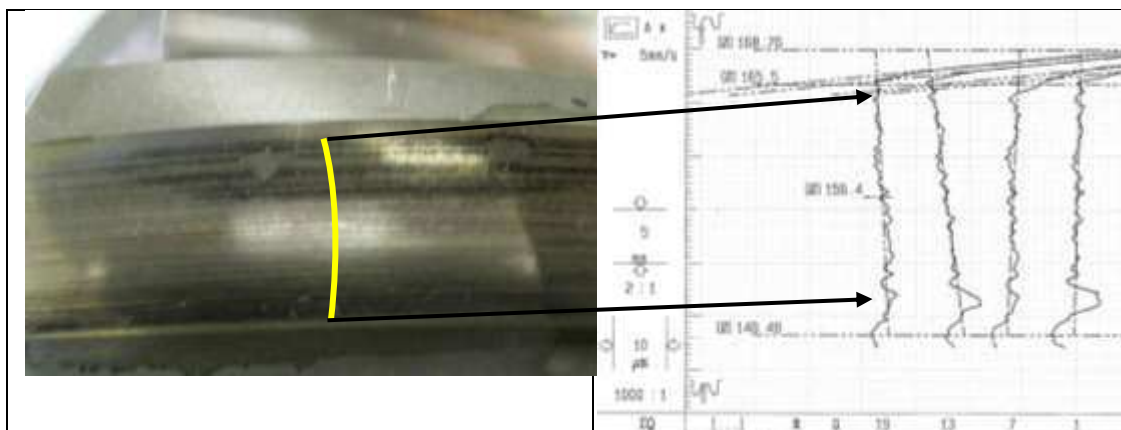
Sequence No.	Cycle No. (millions)	Torque ratio	Contact stress (MPa)	Test results
1	8	0.3	1076	no micropitting
2	8	0.5	1332	initial micropitting
3	8	0.6	1452	slight progression of micropitting
4	8	0.7	1563	very little progression of micropitting
5	8	0.8	1666	increased progression of micropitting
6	8	0.9	1763	micropitting appeared in some areas
7	8	1	1855	micropitting appeared in most areas

5.3 Tooth profile deviation analysis

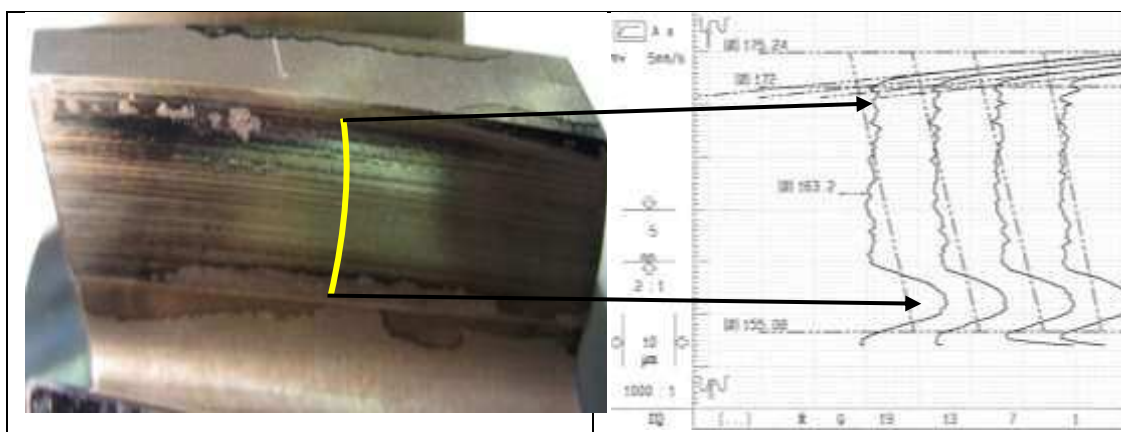
The tooth profile deviation is measured after the test cycle run at the torque ratio of 1.0, after the gear teeth are subjected to the maximum contact stress. At this stage the micropitting spreads over on the most tooth surfaces of gear pair. The tooth surface damage areas of tooth number 1 for the pinion and wheel, as well as the tooth profile deviation measurements for tooth number 1, 7, 13 and 19 are shown in Figure 9 (a) and (b) respectively. The maximum profile deviation of pinion gear occurs at the dedendum, located at diameter 151.5 mm and at diameter 164.3 mm (near the beginning of the tip

relief). Area near the beginning of tip relief of tooth number 7 starts to erode when compared to that of tooth numbers 1, 13 and 19, as shown in Figure 9 (a).

The tooth profile deviation caused by micropitting at the dedendum area of the wheel starts at the start of active profile (SAP) at diameter 155.08 mm, as shown in Figure 9 (b). The deviation of wheel gear teeth is greater and the micropit is deeper than that on the pinion gear. It is clear that the profile deviation of wheel teeth extends from the SAP to the pitch line position (diameter of 163.2 mm), and from the pitch line to the tip circle (diameter of 175.24 mm) of the wheel. This indicates that the micropitting on the driven gear surfaces leads to the loss of the tooth profile from root to tip. This can result in loss of transmission efficiency and increase the level of vibration, which further affects the gear tooth meshing accuracy and causes extra stress concentration on the micropitting area. It is noted that for both gear teeth the micropitting at the dedendum is deeper than that of addendum, causing profile loss, as illustrated by the results of the profile measurement.



(a) Pinion tooth profile deviations



(b) Wheel tooth profile deviations

Figure 9 Tooth profile deviation measurement at the end of the test

5.4 Analytical results using the ISO/TR recommended procedures

The gear tooth contact stress and specific lubricant film thickness are determined at different torque levels. Variations of surface roughness during the test stages are considered in the analysis, based on the surface roughness values obtained from the measurement of tested gears after each cycle run under specific torque ratios. As shown in Figure 10, the contact stress increases proportionally as the torque is increased, and the maximum contact stresses occur at the beginning of the tip relief (point DE, shown in Figure 4 (c)) of the pinion gear, when it meshes with the dedendum of the wheel, and at the area of point AB, with which the beginning of the wheel tip relief meshes. The contact stress results reveal that the micropitting can initiate at the beginning of the tip relief because these areas are subjected to high levels of contact stresses.

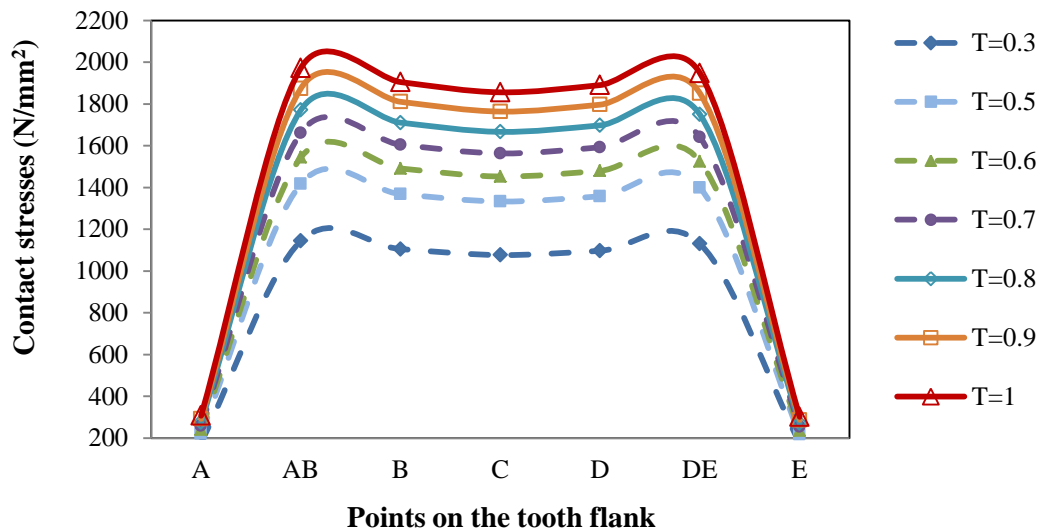


Figure 10 Contact stresses at different torque ratios

As shown in Figure 11, the specific lubricant film thickness varies greatly along the tooth flank during each meshing cycle, and the maximum film thickness occurs at pitch point C because of pure rolling. It shows a considerable variation of the specific lubricant film thickness between the end and the beginning of the tip relief of pinion, point E and DE respectively. The beginning of tip relief, point DE for pinion and point AB for wheel, have a greater risk of micropitting due to lowest lubricant film thicknesses at these regions compared to other contact points. In the analytical calculation, effects of both torque variations and surface roughness changes as measured from the tested pinion gear are considered. The variation of specific lubricant film thickness along the tooth flank between the torque ratio of 0.6 and 1.0 is trivial. This can be attributed to two factors: (1) the tip relief factor used in the calculation is varied for different torque levels however, a specific torque value is used to determine the tip relief factor in the tested gears; (2) the variation of the surface roughness after gears being tested under increased load cycles. It is clear that the variation of surface roughness throughout the test stages

has a greater effect on the specific lubricant film thickness than the increase of torque levels. The considerable variation of lubricant film thickness along the tooth flank during each meshing cycle may also cause the interruption of lubrication resulting in micropitting.

Figure 11 shows that the minimum specific lubricant film thickness at maximum torque ratio of 1.0 is about 0.686 at the addendum of the pinion (point DE) where the tip relief begins and at the dedendum of the pinion (point AB) which meshes with the area of the tip relief of the wheel. Thus, micropitting is most likely to occur in both addendum and dedendum areas. Linke [24] estimated the micropitting risk by specifying the values of the specific film thickness in relation to hardness values of gears, as shown in Figure 12. The Vickers hardness (HV) of the tested gears is 746 (Table 1). As can be seen from Figure 12, the minimum value of the specific lubricant film thickness obtained from the analytical calculation falls into the micropitting region, marked on the Linke curve. The ISO/TR recommended procedures [19, 20] does not provide any recommended values of the minimum safety factor against micropitting risk. The Linke curve may be used to estimate the micropitting risk, by determining the value of specific lubricant film thickness with consideration of surface hardness of the tooth flank. Dudley [1] found if the specific lubricant film thickness was bigger than unity, the gears were in the full lubrication condition. Moreover, according to Kissling [25], the minimum micropitting safety factor should be greater or equal to unity. The micropitting safety factor based on the film thickness value obtained in this study is less than unity especially when loaded under higher torque ratios. The gear test results have confirmed that the micropitting has initiated and propagated then spreaded out over the addendum and dedendum of the tooth flanks, as summarised in Table 3.

According to the analytical results, the maximum contact stresses and minimum specific film thicknesses occur at the addendum and dedendum of the pinion, as shown in Figures 10 and 11. Based on the experimental results, the micropitting occurs in these areas too. Thus, the micropitting may be predicted, by applying the analytical procedure based on the ISO/TR recommended procedures [19, 20], if detailed measurements of surface roughness and profile modifications are available. From this study, it is clear that the excessive load, micro-geometry, surface roughness and lubricant film thickness are the main influence factors of micropitting initiation and propagation.

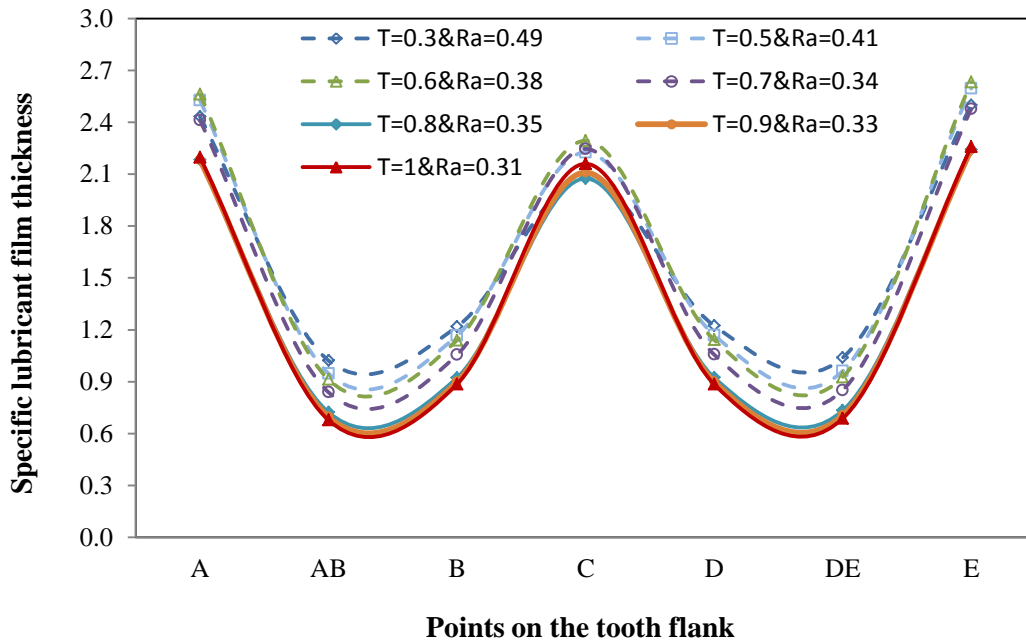


Figure 11 Specific lubricant film thicknesses at different torque and surface roughness values

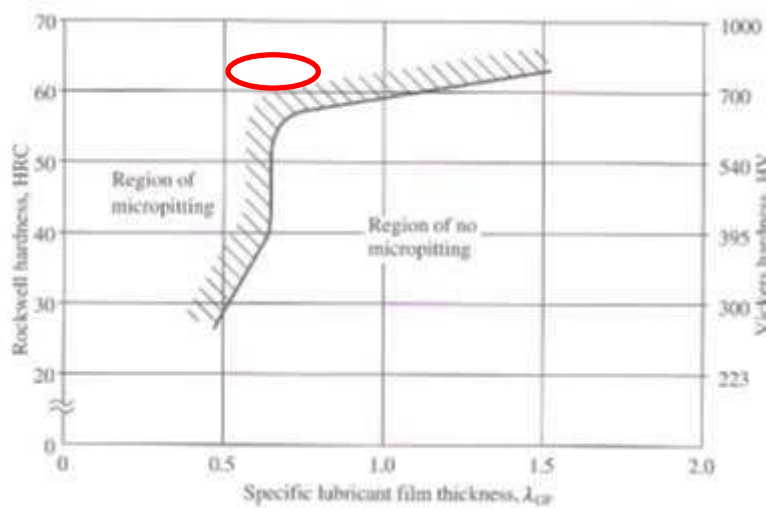


Figure 12 Prediction of micropitting risk by specific film thickness and gear hardness [24]

6. Conclusions

Experimental and analytical studies have been undertaken to investigate micropitting initiation and propagation under varying torque levels. It has found that the excessive loading, micro-geometry, surface roughness and lubricant film thickness are the main factors affecting micropitting. From the results obtained, the following conclusions can be drawn:

- Micropitting starts to occur at the torque ratio of 0.5 in the dedendum area of pinion. This micropitting is non-progressive, and remains in the dedendum area until the final test run. However, the micropitting also prevails at the pinion addendum, owing to progressive micropitting at the dedendum of the wheel.
- The micropitting at the pinion dedendum is less severe than at the addendum area, but pits are deeper at the dedendum, according to the profile deviation results. This indicates that the micropitting on the pinion dedendum has caused the profile deviation.
- The tooth profile deviation of wheel gear is worse and micropitting is more progressive than that of the pinion gear. The wheel profile deviation appears from the root to the tip of the wheel. The beginning edge of the pinion tip relief can contribute to the initiation of micropitting at the dedendum of the wheel.
- The analytical results show that the maximum contact stresses and minimum specific film thickness occur at both addendum and dedendum of the pinion and wheel; the grinding cutting edges due to the tip relief of gear tooth profiles contribute to the micropitting initiation and propagation in these areas.
- Compared to the experimental results, the analytical calculation based on ISO/TR15144-1:2010 and ISO/TR15144-1:2014 shows a correlation between the predicted minimum specific lubricant film thickness and the occurrence of micropitting observed in the experiment.

Nomenclature

Symbol	Description	Units
b	Face width	mm
C_a	Tip relief	μm
C_{eff}	Effective tip relief	μm
F_t	Tangential load	N
G_M	Material parameter	-
h_Y	Local lubricant film thickness	μm
K_A	Load application factor	-
$K_{H\alpha}$	Transverse load factor	-
$K_{H\beta}$	Face load factor	-
K_v	Load dynamic factor	-
$p_{dyn,Y}$	Local Hertzian contact stress	N/mm^2
R_a	Effective arithmetic mean roughness value	μm

R_z	Mean of the height of five peaks to valleys	μm
$S_{GF,Y}$	Local sliding parameter	-
U_Y	Local velocity parameter	-
W_Y	Local load parameter	-
Z_E	Elasticity factor	$(\text{N}/\text{mm}^2)^{0.5}$
α_t	Transverse pressure angle	degree
β_b	Base helix angle	degree
$\lambda_{GF,min}$	Minimum specific lubricant film thickness	-
$\lambda_{GF,Y}$	Local specific lubricant film thickness	-
λ_{GFP}	Permissible lubricant film thickness	-
$\rho_{n,Y}$	Normal radius of relative curvature at point Y	mm

References

- [1] D.W. Dudley, Handbook of Practical Gear Design, CRC Press. 1994.
- [2] P.J.L. Fernandes and C. McDuling, Surface contact fatigue failures in gears. Engineering Failure Analysis 4(2) (1997) 99-107.
- [3] R.L. Errichello, Morphology of micropitting. The Journal of Gear Technology (2012) 74-81.
- [4] J. Zhang, Influence of Shot Peening and Surface Finish on the Fatigue of Gears. PhD Thesis, University of Newcastle upon Tyne, 2005.
- [5] S. Krishnamurthy and A.R. Rao, Effect of sursulf treatment on the performance of 0.14% C steel gears. Wear 120(3) (1987) 289-303.
- [6] P. Brechot, A.B. Cardis, W.R. Murphy, J. Theissen, Micropitting resistant industrial gear oils with balanced performance. Industrial Lubrication Tribology, 52(3) (2000) 125-136.
- [7] J. Zhang and B.A. Shaw, The effect of superfinishing on the contact fatigue of case carburised gears. Applied Mechanics and Materials, 86 (2011) 348-351.
- [8] W. Predki, K. Nazifi, G. Lutzig, Micropitting of big gearboxes: Influence of Flank Modification and Surface Roughness. Gear Technology. 2011(May 2011):42-46.
- [9] M.A. Muraro, F. Koda, et al, The influence of contact stress distribution and specific film thickness on the wear of spur gears during pitting tests. Journal of the Brazilian Society of Mechanical Sciences and Engineering. 34(2) (2012) 135-144.
- [10] V. Moorthy, B.A. Shaw, Effect of as-ground surface and the BALINIT C and Nb-S coatings on contact fatigue damage in gears. Tribology International, 51(2012) 61-70.

- [11] H.P. Evans, R.W. Snidle, K.J. Sharif, B.A. Shaw, J. Zhang, Analysis of Micro-Elastohydrodynamic Lubrication and Prediction of Surface Fatigue Damage in Micropitting Tests on Helical Gears. *Journal of Tribology*, 135(1) (2013) 1-9.
- [12] B.R. Hohn, K. Michaelis, Influence of Oil Temperature on Gear Failures. *Tribology International*, 37(2) (2004) 103-109.
- [13] A. Oila, S.J. Bull. Phase transformations associated with micropitting in rolling/sliding contacts. *Journal Materials Science*. 40(18) (2005) 4767-4774.
- [14] E. Lainé, A.V. Olver, T.A. Beveridge, Effect of Lubricants on Micropitting and Wear. *Tribology International*, 41(2008) 1049-1055.
- [15] J. Kleemola, A. Lehtovaara, Experimental Simulation of Gear Contact along the Line of Action. *Tribology International*. 42(10) (2009) 1453-1459.
- [16] M.J.A. Holmes, H.P. Evans, R.W. Snidle, Analysis of Mixed Lubrication Effects in Simulated Gear Tooth Contacts. *Journal of Tribology*. 127 (2005) 61-9.
- [17] J.A. Brandão, J.H.O. Seabra, J. Castro, Surface initiated tooth flank damage. Part II: Prediction of micropitting initiation and mass loss. *Wear*, 268(1) (2010) 13-22.
- [18] D. Zhu, Q.J. Wang, Effect of Roughness Orientation on the Elastohydrodynamic Lubrication Film Thickness. *Journal of Tribology*. 135 (2013) 1-9.
- [19] ISO/TR 15144-1:2010 Calculation of Micro-pitting Load Capacity of Cylindrical Spur and Helical Gears — Part 1: Introduction and Basic Principles. BSI Standard Publication. 1-56.
- [20] ISO/TR 15144-1:2014 Calculation of Micro-pitting Load Capacity of Cylindrical Spur and Helical Gears. Introduction and Basic Principles. BSI Standard Publication. 1-35.
- [21] V. Moorthy, B. A. Shaw, Contact Fatigue Performance of Helical Gears with Surface Coatings. *Wear*, 276-277 (2012) 130-140.
- [22] ISO 6336-1. Calculation of Load Capacity of Spur and Helical Gears Part 1: Basic Principles, Introduction and General Influence Factors. 2006, U.K: BSI, 1-109.
- [23] R.W. Snidle, H.P. Evans, M.P. Alanou, M.J.A. Holmes, Understanding Scuffing and Micropitting of Gears. NATO Research and Technology Organization Specialists' Meeting on The Control and Reduction of Wear in Military Platforms (RTO-MP), (2004)1-18.
- [24] D. Jelaska, *Gears and Gear Drives*. Sussex: Wiley; 2012.
- [25] U. Kissling, Application of the First International Calculation Method for Micropitting. *GearTechnology*, (2012) 54-60.